COBEM 2021 26th International Congress of Mechanical Engineering
ABCM Associação Brasileira de Engenharia e Ciências Mecânicas
November 22-26, 2021, Virtual Congress, Brazil

COB-2021-0553
Evaluation of the use of parallel kinematic mechanisms for robotic human wrist

Thales Travaglini Galanti
Chi Nan Pai
Polytechnic School of the University of Sao Paulo, Department of Mechatronic and Mechanical Systems Engineering, Sao Paulo, Brazil
ttravaglinigalanti@usp.br, chinan.pai@usp.br

Abstract. *Robotic upper limbs have been researched for several applications, such as biomechanical prosthesis, parts of an android, robotic cookers, etc. Among all the joints of the human upper limb, the wrist joint stands out as an extremely difficult one to be replicated by using conventional motors. This is because it presents two rotational movements with the same rotational center, which is almost impossible to be replicated by using rotary motors. In the present work, we evaluated the use of parallel kinematic mechanisms to replicate the movements of the human wrist, which are: flexion/extension and adduction/abduction of the hand, and the combination of both, called circumduction. Three designs were evaluated. Two of them use three linear actuators, and the third one uses four linear actuators. The fundamental difference between the first two designs is the position of the rotational center, which is also the center of movement of the hand. In the first one, the center is located at the barycenter of the equilateral triangle formed by the linear actuators, while in the second one it is located at the intersection between two orthogonal planes, where one plane contains one actuator and is equidistant to the others two, and one plane is located equidistant to all three actuators. A computer-aided design (CAD) software was used to simulate the movements of all mechanisms, and mechanical equations were delivered from the CAD model to calculate the rotational angles and the output torques. As a result, the first two mechanisms present a total angular variation of 43.6 degrees and a torque of 1 Nm for adduction/abduction, 49.6 degrees and a torque of 1.15 Nm and 1.3 NM for flexion/extension. The first one presented a little displacement of the rotational center in the axial direction, while there is no variation in the position of the rotational center in the second mechanism. The third mechanism, with four linear actuators, achieved 38 degrees of total angular rotation in both adduction/abduction and flexion/extension, with a torque of 1.16 Nm. Therefore, for the movement of adduction/abduction, our designs achieved, respectively, 67.1 % and 58.46 % of the angular movement of the human wrist, and for the movement of flexion/extension, 33.1 % and 25.3 % of the human wrist.*

Keywords: *Robotic upper limb, artificial wrist, parallel kinematic mechanism, biomechanic, linear actuator*

1. INTRODUCTION

The absence of a limb represents a significant impact on a patient's life. Especially if it is an upper limb and it was lost during adult age. To solve this problem, several groups have been researching upper limb prostheses. One part of the upper limb that has shown to be challenging for the design of the prosthesis is the wrist. This is because it combines two orthogonal rotations in one single center, being responsible for the movements of flexion/extension and adduction/abduction of the hand.

In the literature, it is possible to find designs of humanoid or robotic arms with interesting wrists mechanisms, like iCub (Parmiggiani *et al.* (2012)) and ShadowHand (ShadowRobotCompany (2020)). The iCub uses two rotational motors connected to a complex mechanism to perform two orthogonal rotations with the same center, while the ShadowHand uses big linear actuators, located in the forearm, to generate the moments, which makes the size of the device bigger than the average size of a human forearm.

Other groups have been focusing only on the development and the analysis of robotic wrists. Some of them like Penčić *et al.* (2018) and Albers *et al.* (2010) achieved interesting mechanisms, but their devices also presented the same problems of a complex and big system, which make their use in a prosthesis impossible. Furthermore, the Bajaj *et al.* (2019) analyzed different designs of wrists and divided them according to the degrees of freedom (DOF). The most promising one is a parallel mechanism with 2-DOF. But, again, it is very big and complex.

An interesting solution was the one proposed in the R1 robot wrist (Sureshbabu *et al.* (2017)), where a parallel kinematic mechanism was used. Three rotational motors are located in the forearm and their rotational movements are converted into linear ones through threaded shafts. All three sharts are connected to a platform that simulates the movements of a human wrist joint. This mechanism is interesting because it allows flexion/extension, adduction/abduction and cir-

cumduction with the same center of movement using the principle of linear motion. Although the R1 presented an interesting solution, the implementation of this mechanism used all the space available in the forearm, which leaves no space for the fixation of motors responsible for the movements of the hand.

The objective of this work is to evaluate the use of parallel kinematic mechanisms with linear motors as a compact system to simulate the movements of a human wrist. Three different ideas will be evaluated. The first one has three linear actuators positioned at the vertices of an imaginary equilateral triangle, and the center of the wrist joint located at the triangle barycenter. The advantages of this configuration are symmetry and easy sizing. The second one is similar to the first one, but the joint center is located at a half distance of the height of the triangle, instead of the barycenter. In this configuration, the movements of flexion/extension and adduction/abduction will occur at the same distance to all three motors. Finally, the third solution explores the same principles by using four linear motors, which makes the design simpler, but increases the overall size of the system.

2. MATERIALS AND METHODS

2.1 Linear motors and their positions

The R1 robot used three linear motors for the wrist mechanism, as well as our first two designs. All three motors were positioned in an equidistant way, so each actuator would be at the vertices of an equilateral imaginary triangle. In our design, we chose to put one motor in the ventral position and the others two in the dorsal position. In this configuration, the movement of flexion and extension will be performed by, respectively, the extension and the retraction of the two dorsal actuators, and the retraction and the extension of the ventral actuator, (Image 1a). For the movement of adduction and abduction, the ventral motor will be at its original position, while the two dorsal motors will move in opposite directions, (Image 1b). This configuration was chosen to prioritize the movement of flexion/extension over the movement of adduction/abduction. Figure 1 shows the mechanism and the movements: linear motors, illustrated in black, are placed in a triangular position, while the wrist joint mechanism is shown in blue.

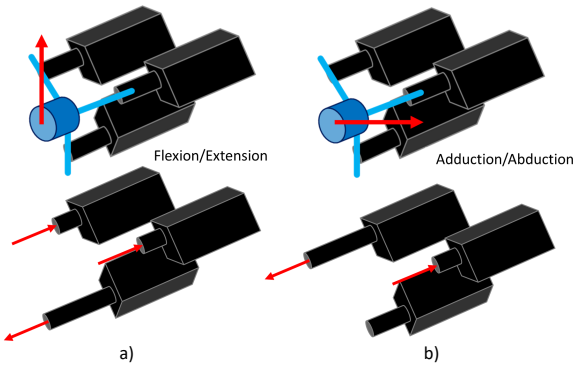

Figure 1. Representation of the extension and compression of the engine motors to perform the movements. a) flexion/extension; b) adduction/abduction

The size of the equilateral triangle was defined to be up to 50 mm, because it can be positioned inside an ellipse that simulates an adult human wrist, with 60 mm as the major axis and 40 mm as the minor axis.

The linear motors (PQ-12, Actuonix Motion Devices Inc., Canada) chosen for this work has 48 mm in length, 21.55 mm in height and 15 mm in thickness, with a total stroke length of 20 mm. The peak efficiency point of this motor is 20 N.

2.2 Numerical evaluations

2.2.1 Flexion/Extension angle

In our design, all shafts of the motors will initially be extended 10 mm, a configuration defined as the rest position, as shown in Figure 2a. One can see the equilateral triangle, shown in gray lines, and the height of the triangle, segment AB, shown as a yellow line. During the movement of extension, one motor will extent its shaft up to 10 mm, while the other two motors will retract their shafts up to 10 mm, as shown in Figure 2b. In this case, a new segment A'B' (red line) will be formed. The angle between AB and A'B' is the angle for flexion/extension, as shown in Figure 2c). Therefore, an equation $\beta = arctan(\frac{AA'}{x})$ can be derived, where x is the side of the imaginary equilateral triangle and AA' is the 10 mm variation of the motor stroke.

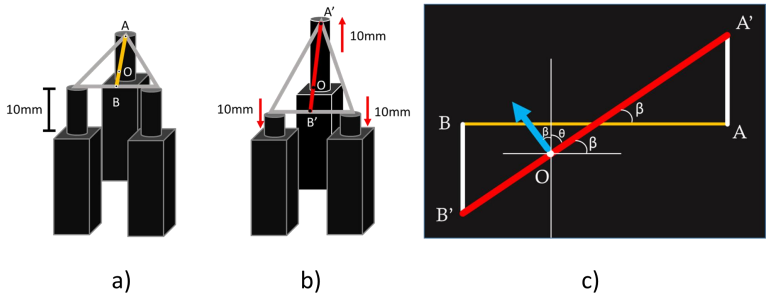

Figure 2. a) rest position; b) movement of flexion/extension and c) its angle

2.2.2 Adduction/Abduction angle

For the movement of adduction/abduction, the ventral motor stays at the rest position and the dorsal motors realize an opposing movement. In the rest position, one can find a segment CD between the dorsal actuators, which is the side of an imaginary equilateral triangle, as shown in the schematic of Figure 3a). When one of the motors makes a retraction movement of up to 10 mm, the other is making an extension of the same length. Therefore, the distance between the extremity of the strokes would be C'D', as shown in Figure 3b. Thereby, the angle α between CD and C'D' represents the adduction/abduction angle, which is defined by the equation $\alpha = arctan(\frac{2 \times \overline{DD'}}{x})$, with DD' representing the stroke variation and x the side of the imaginary equilateral triangle.

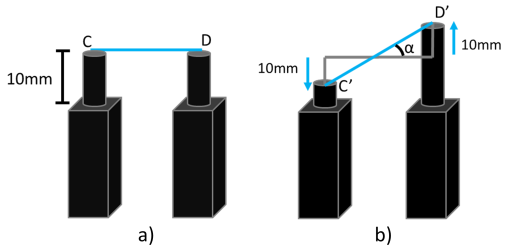

Figure 3. a) rest position; b) movement of adduction/abduction and its angle

2.2.3 Flexion/Extension torque

Figure 4 shows the schematic used for the calculation of the torque of flexion/extension. We assumed that the axis of the torque will pass through the barycenter, denominated as point "O". The segment D1 would be the distance between the point "O" and the line connecting both motors at the dorsal position, and the segment D2 would be the distance between the point "O" and the motor at the ventral position. In Figure 4, the dorsal actuators are retracting their shafts (F1 and F2 forces entering the plane of the paper) and the ventral motor is extending (F3 force exiting). This represents the extension of the wrist, and the torque around the axis x would be $|M| = 2 \times F \times D2$, where F is the linear force of PQ-12 Actuonix motor of 20 N and D2 is two times D1 of the triangle height.

2.2.4 Adduction/Abduction torque

The torque for adduction/abduction is generated by both motors at the dorsal position, as shown in Figure 5. In the schematic, one force F1 is exiting and the other force F2 is entering the plane of the paper. By assuming the distance D as half of the side of the triangle, the torque would be $|M| = 2 \times F \times D$.

2.3 Evaluation criteria for the performace and the positioning of the motors

The first parameter used to evaluate the mechanisms is the angle value of the movements. According to Chim (2017), the movement of flexion/extension has a range of 150º (75º for each side), 45º for adduction and 20º for abduction. The second parameter is the torque value of the movement. The minimum torque would be the one enough to move the hand,

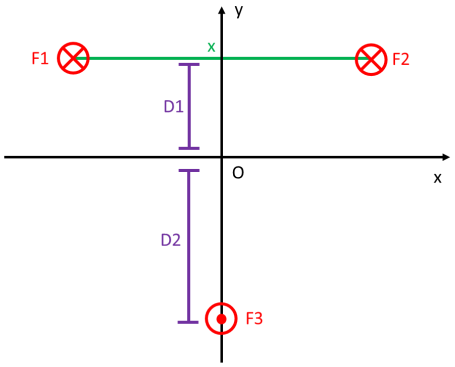

Figure 4. Schematic for calculation of torque during the movement of flexion/extension

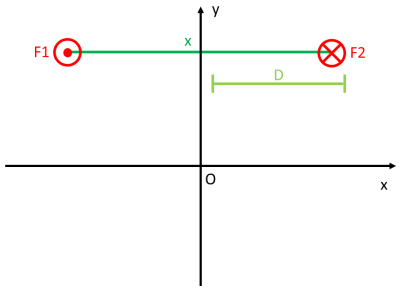

Figure 5. Schematic for calculation of torque during the movement of adduction/abduction

with an estimated mass of 500 g. By assuming that the center of the hand is located 100 mm from the wrist, the minimum torque would be 0.5 Nm. This desired parameter was used for movements of flexion/extension and adduction/abduction.

The last consideration is about the size of the imaginary equilateral triangle. We discussed before that the maximum size would be 50 mm. We explored the other options, with 40 mm and 30 mm as the size of the equilateral triangle.

2.4 Design of the wrist joint

The human wrist joint is composed of several bones responsible for the connection between the hand and the forearm. A similar mechanism was designed for the same function, as shown in Figure 1. The blue piece contains a central part connected to three rods.

In our first design of the wrist mechanism, the central part is located at the barycenter of the imaginary triangle, while the rods extend to each linear motor. The hand is supposed to be attached to the central part of this mechanism. During the movement of flexion/extension, the position of the central part would change, as illustrated in Figure 2c. The point "O" changed from a plane that contains the segment AB to a plane below. The point "O" is supposed to be fixed, because it represents the rotational center of the movements flexion/extension and adduction/abduction. The variation of its location may influence the position of the tip of the fingers, which will affect the precision of the movements.

In our second design of the wrist mechanism, the central part is located at half the height of the triangle. In this configuration, the point "O" is not moved by the flexion/extension or the adduction/abduction, because it is at the intersection between the segments AB and A'B', as shown in Figure 2c.

2.4.1 Connecting mechanism between the motors and the wrist joint

Another important part of the wrist joint is the connection between the rods and the shaft of the linear motors. This is important because the movement of the shaft of the motors rotates the angle of the plane that contains the surface of the central part. As consequence, there is a change in the distance between the tip of the motor shaft and the central part.

To solve this problem of variation of distance, we designed a ring that allowed the cylindrical rod to move linearly inside, compensating for the change in the distance. Figure 6 shows the schematic of this compensation. Other problems are related to the rotation of the mechanism. A structure in ring shape allows the rotation of the cylindrical rod inside. This rotation is defined as ωy. The ring should be able to rotate around the other two axes as well, defined as ωx and ωz. These rotations were achieved by connecting the ring to a structure in "U" shape through two little shafts, and connecting the "U" shape structure to the base through a vertical shaft.

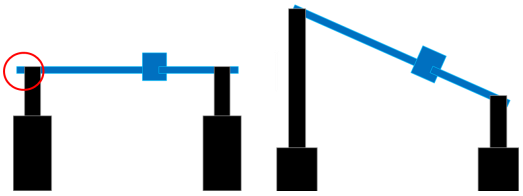

Figure 6. Scheme showing linear displacement

2.5 Wrist mechanism with four linear motors

Our third design uses four linear motors instead of three. This configuration was considered because of the symmetry in two planes, which makes the mechanism very easy to understand and to design. This configuration, as shown in Figure 7a, would provide higher torque and maybe bigger angular variation. The main disadvantage of this design would be the overall size of this mechanism.

To fit this mechanism inside the domain of an ellipse, as described before, it was found that the maximum distance between the center of the square and the tip of the linear motors is 20.5 mm, as shown in Figure 7b.

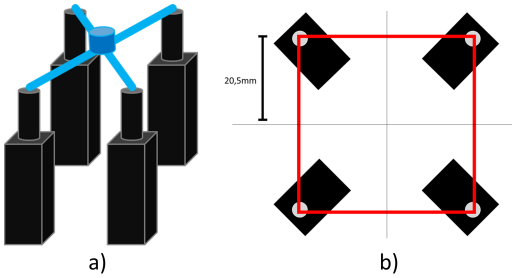

Figure 7. On the left the wrist mechanism with four motors and on the right the model with distance

Figure 8 shows the forces responsible for flexion/extension and adduction/abduction. The linear motors need to operate in pairs, as F1 and F2 (in red) and in F1' and F2' (in green) to perform these movements.

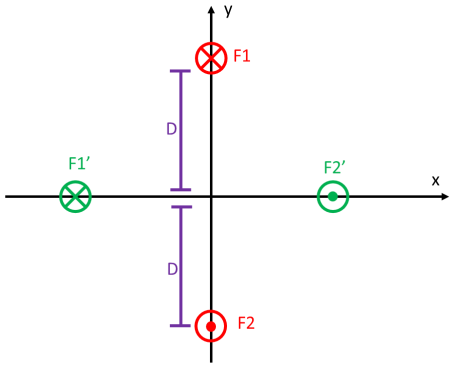

Figure 8. Force scheme for four motors

Using the same logic as three motors the equation for torque $|M| = 2 \times D \times F$ was derived, where D = 29 mm and F = 20 N. This configuration allows only one possible torque, $|M| = 1.16$ Nm for flexion/extension and adduction/abduction. As for angular variation, the equation $\theta = arctan(\frac{h}{D})$ can also be derived, where h is equal to 10 mm (motor stroke variation), and the value of 19º for both movements.

3. RESULTS

3.1 Location of the linear motors

Based on the equations derived for angular variation and torque, Table 1 summarizes the different values of angles and torques for different sizes of the equilateral triangle.

Table 1. Comparison between angle and torque values, for possible sizes of the imaginary equilateral triangle

Specifications	**Desired values**	**30 mm**	**40mm**	**50mm**
Adduction/Abduction Angle	45º/20º	33,7º	26,6º	21,8º
Flexion/Extension Angle	75º	37,6º	30º	24,8º
Adduction/Abduction Torque (Nm)	>0.5	0,6	0,8	1
Flexion/Extension Torque (Nm)	>0.5	0,69	0,92	1,15

It is possible to see, from the Table 1, the opposing effect between the angles and the torque; the increase of one leads to decrease of the other. Since all the angles were below the desired ones, the torque values were used as the parameter of choice. Therefore, the 50 mm configuration was chosen for the development of the three motors system configurations and the basis to achieve an equivalent four motors wrist mechanism.

3.2 Development of the motor-joint connection mechanism

Figure 9 shows the mechanism designed to connect the wrist joint mechanism to the shaft of the linear motor. The ring, as shown in yellow, has an internal diameter of 5 mm, where could pass a cylindrical rod with the freedom to perform relative linear (ly) and angular (ωy) movement. This ring is attached to a "U" shape structure by two shafts, allowing the ωx rotation. Finally, the "U" part is connected to a base by a cylindrical shaft, which enables the ωz rotation.

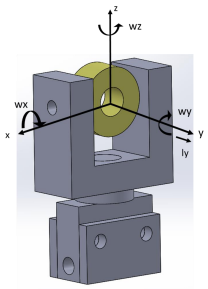

Figure 9. Motor-joint connection mechanism

3.3 Development and performance validation of the kinematic parallel mechanism

Figure 10 shows the three designs of the wrist mechanism in their rest position. In the first two designs, all three motors are places in an equilateral triangle with 50 mm of side, while the third design has four motors located at the vertices of a square with 41 mm of side.

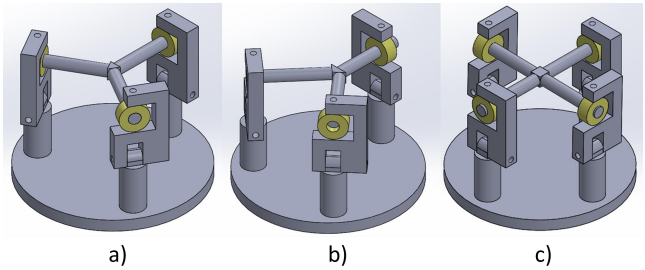

Figure 10. Parallel kinematic mechanisms: a) center of the joint in the barycenter; b) center displaced; c) four motors

Figure 11a shows an example of movement of flexion/extension, while the Figure 11b shows an example of the movements of adduction/abduction. The motor-joint connection mechanism shown in Figures 10 and 11 are not the final version shown in Figure 9. However, the principle of both mechanisms is the same. The final version was designed to simplify the manufacturing process.

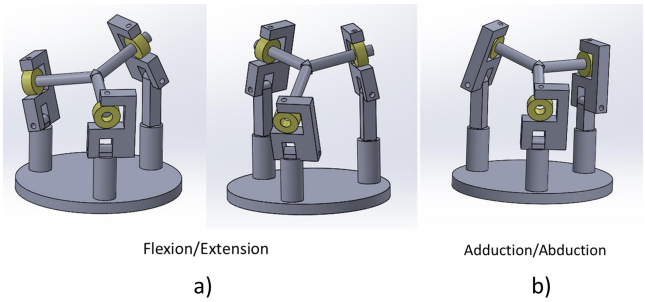

Figure 11. Movements of the parallel kinematic mechanism: a) flexion/extension; b) adduction/abduction

3.4 Wrist mechanisms and analysis

With the validation of the parallel kinematic mechanism became plausible to make the wrists prototyping. In the Figure 12, for three motors 12a is the model with the center of the joint in the barycenter and 12b the system with the center displaced to half the height, and in 12c the case for four actuators.

In general, the systems have a superior disco, with 75 mm in diameter, responsible to fix the motors and allowing that the motors courses stay external, so making possible the extension and retreatment of course. Distant 40 mm exist and connected through four axes exist an inferior disco, with 80 mm, he is responsible to support another piece with 9 mm thickness which regulates the position of the motor and let the actuators fixed.

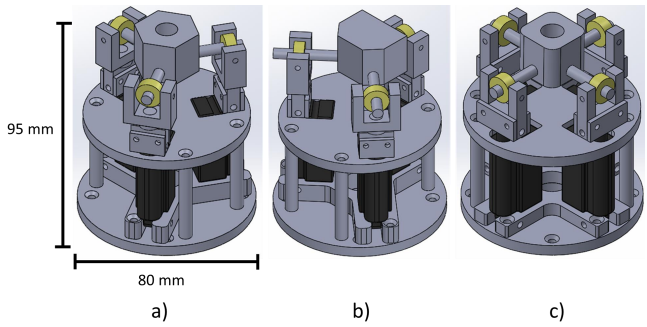

Figure 12. Wrists mechanisms

For the first mechanism, the center of the wrist joint has a hexagonal form with three equal rods, because how the center of mass is in the barycenter of the imaginary triangle the angle between the rods is 120º so it was possible to explore this symmetry. The second project has the center displaced and this allows that he doesn't have a relative movement, but this change turns the sizing a little complicated, because will be necessary two bigger dorsal rods, the angle between them is 90.2º, and a third ventral and smaller, in the joint. These features demanded more attention to the sizing because all the pieces need to have this angle to make the fixing and allowing the mechanism operation, this also impacts the center of the joint, having a specific form. For the four motors wrist mechanism is more simple, the center has a square form and he won't have a relative movement because of the symmetry of form and motion with two couple of actuators doing the same process but one pair making flexion/extension and another adduction/abduction.

In possession of the wrists mechanisms developed, was possible to test the movements of the system. In the Figure 13 was coupled a representative hand and can see the reflection of the wrist movement in the hand, in the left is the adduction/abduction and in the right the flexion/extension. So how these motions happen independently in the same mechanism, they could be combined in the circulation movement.

To finish the wrist mechanisms analysis was constructed the Table 2 comparing the performance between the three systems. One first contestation is the devices couldn't achieve the angular variation intended values and to improve it would be necessary to decrease the torque. Another observation is even with four motors the torque values for flexion/extension were inferior concerning the three actuators system because for three motors all of them work to move, while in the other case only two are used. In the same logic, the angle values for four motors are smaller, because the arm of action between the center of the joint and the motor is bigger than for three actuators, decreasing the angular variation. Noteworthy, despite the four motor mechanisms, don't have the expected performance, he still possesses a relevant symmetry and this helps to make the movements equally. For three actuators the values are practically equal for both cases and the difference

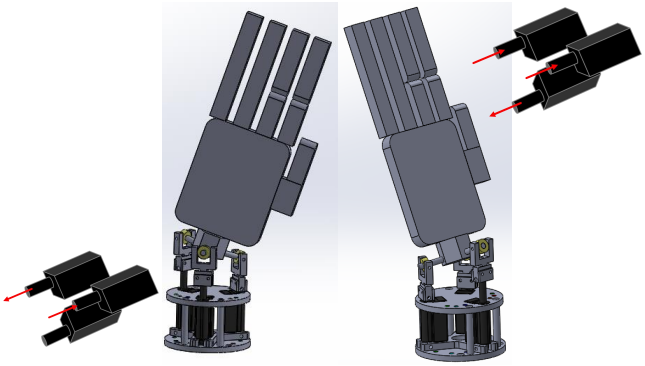

Figure 13. Motion validation

consists in avoiding the center displacement, consequently preventing an unwanted hand displacement, but for this, it's needed to pass through sizing difficulties. In sequence, the designs with three motors achieved 67.1 % and with four motors 58.46 % of the adduction/abduction movement of the human wrist, and for flexion/extension, 33.1 % and 25.3 % of the human wrist.

Table 2. Performance comparison between wrist mechanisms

Specifications	**Intended**	**Center of mass in the barycenter for 3 Motors**	**Displaced center of mass for 3 Motors**	**4 motors**
Adduction/Abduction Angle	45º/20º	21.8º	21.8	19
Flexion/Extension Angle	75º	24.8º	24.8	19
Adduction/Abduction Torque (Nm)	>0.5	1	1	1.16
Flexion/Extension Torque (Nm)	>0.5	1.15	1.299	1.16

4. CONCLUSION

In this work, three wrist mechanisms based on the parallel kinematic system were presented and evaluated. The first design uses three motors located at the vertices of an equilateral triangle, and the wrist joint is located at the barycenter of the triangle. The second design used the same three motors, but the wrist joint is located at half the height of the triangle. The third design uses four linear motors instead of three, to form a square, with the wrist joint located at the center of the square. After evaluations, the second design was considered the best for our purpose because of the small overall size, compared to the third design, the higher precision in the movement of the hand, and better angular variation and torque. As future work, prototypes of all three designs are going to be made for experimental evaluation and confirmation of the numerical analysis, and a prototype of a robotic arm using the second design of the wrist will be developed.

5. BIBLIOGRAPHY

Albers, A., Sander, C. and Simsek, A., 2010. "Development of the actuation of a new wrist for the next generation of the humanoid robot armar". In *2010 10th IEEE-RAS International Conference on Humanoid Robots*. IEEE, pp. 677–682.

Bajaj, N.M., Spiers, A.J. and Dollar, A.M., 2019. "State of the art in artificial wrists: a review of prosthetic and robotic wrist design". *IEEE Transactions on Robotics*, Vol. 35, No. 1, pp. 261–277.

Chim, H., 2017. "Hand and wrist anatomy and biomechanics: A comprehensive guide". *Plastic and reconstructive surgery*, Vol. 140, No. 4, p. 865.

Parmiggiani, A., Maggiali, M., Natale, L., Nori, F., Schmitz, A., Tsagarakis, N., Victor, J.S., Becchi, F., Sandini, G. and Metta, G., 2012. "The design of the icub humanoid robot". *International journal of humanoid robotics*, Vol. 9, No. 04, p. 1250027.

Penčić, M., Rackov, M., Čavić, M., Kiss, I. and Cioată, V., 2018. "Social humanoid robot sara: development of the wrist mechanism". In *IOP Conference Series: Materials Science and Engineering*. IOP Publishing, Vol. 294, p. 012079.

ShadowRobotCompany, 2020. "Dexterous hand series: The world's most dexterous humanoid robot hands". URL `https://www.shadowrobot.com/dexterous-hand-series`.

Sureshbabu, A.V., Chang, J.H., Fiorio, L., Scalzo, A., Metta, G. and Parmiggiani, A., 2017. "A parallel kinematic wrist for the r1 humanoid robot". In *2017 IEEE International Conference on Advanced Intelligent Mechatronics (AIM)*. IEEE, pp. 1215–1220.